Role of Hartree−Fock and Kohn−Sham Orbitals in the Basis Set Superposition Error for Systems Linked by Hydrogen Bonds

Jorge Garza,* José-Zeferino Ramírez, and Rubicelia Vargas

Departamento de Química, División de Ciencias Básicas e Ingeniería, Universidad Autónoma Metropolitana-Iztapalapa, San Rafael Atlixco 186, Col. Vicentina, Iztapalapa, C. P. 09340. México D. F., México

Received: August 4, 2004; In Final Form: November 11, 2004

In this work the effect of the basis set superposition error (BSSE) is explored with the counterpoise method on the occupied and unoccupied Hartree−Fock (HF) and Kohn−Sham (KS) orbitals. Three different systems linked by hydrogen bonds, $H_2O\cdots FH$, $H_2O\cdots H_2O$, and $H_2O\cdots CFH_3$, were studied by using the basis set families cc-pVXZ and aug-cc-pVXZ (X = D, T, Q). The basis sets were tested with the HF method and two approximations for the exchange−correlation functional of KS: a generalized gradient approximation and a hybrid approach. In addition to these methods, the second-order Møller−Plesset perturbation theory, MP2, was considered. It was found that the presence of the "ghost" basis set affects the orbitals in two ways: (1) The occupied KS orbitals are more sensitive to the presence of this "ghost" basis set than the occupied HF orbitals. For this reason the BSSE observed in HF is less than that obtained with KS. (2) The unoccupied HF orbitals are more sensitive to the presence of the "ghost" basis set than their corresponding occupied orbitals. Because the MP2 method uses both, occupied and unoccupied HF orbitals, to compute the total energy, the contribution of the BSSE is bigger than that obtained with HF or KS methodologies.

I. Introduction

Currently, the quantum chemistry approaches used to estimate the strength of a hydrogen bond in systems of medium size with Gaussian basis set functions are the Møller−Plesset perturbation theory (MP2)[1] and the Kohn−Sham (KS) density functional theory.[2] These methods have in common that they are based on the orbital concept. It is well-known that the MP2 approach takes as the starting point the Hartree−Fock (HF) method,[1] using the occupied and unoccupied orbitals to estimate the correlation contribution missed in HF. Contrary to MP2, in the HF and KS approaches just information of the occupied orbitals is used to evaluate the total energy.

It has been discussed that the HF and KS orbitals are different because they exhibit a different potential in the integral−differential equations involved in both methods.[3,4] Whereas the self-interaction contribution is canceled correctly within HF equations for the occupied orbitals, this contribution is not annulled for the unoccupied orbitals. The KS orbitals show a different behavior, although the self-interaction contribution is not canceled for many of the exchange−correlation functionals frequently used; the local-multiplicative potential involved in the KS equations is the same for occupied and unoccupied orbitals. This difference between HF and KS potentials gives as a result that the energy of the highest occupied molecular orbital (HOMO) is deeper for HF than that obtained with the KS method. However, this is not true for the lowest unoccupied molecular orbital (LUMO), because the KS equations give a deeper LUMO energy with respect to that obtained with HF method.[5]

On the other hand, it has been recognized for many years that the basis set superposition error (BSSE) must be considered when molecular complexes are obtained from two or more species. For this reason several approaches have been proposed to correct such error. Between these approaches the counterpoise (CP) method is the most popular that has been used for many years.[6−8] New approaches have been proposed, but in general the results obtained by these new proposals coincide with those obtained by the CP method.[9−14]

Additionally, the HF, KS, and MP2 approaches are widely used with the CP as the methodology to correct the BSSE. There are several works where comparative studies between these approaches have been performed, the systems linked by hydrogen bonds being the principal target to make such a comparison.[15−18] Analyzing the results reported in the literature, we want to draw three conclusions: (a) If the size of the basis set is small, the BSSE will be large, but the BSSE will decrease if a bigger basis set is used. In fact, in the complete basis set (CBS) limit this error will be zero; however, in practical problems one has to use a truncated basis set, and, consequently, the BSSE is always present. (b) Systems stabilized by strong hydrogen bonds are described in the same way with KS or MP2, but if the hydrogen bond is weak, large discrepancies can be found between both methods. The inclusion of the BSSE on this kind of system is mandatory. (c) The BSSE obtained with HF, KS, or MP2 is different between each method even when the same basis set is used. In general, when a medium or large basis set is used, the BSSE follows the following order: $BSSE_{MP2} > BSSE_{KS} > BSSE_{HF}$.

In this work we explore an explanation of the last conclusion and show why the HF BSSE is less than the KS BSSE. We relate this explanation with the HF and KS orbitals in systems that exhibit hydrogen bonds such as $H_2O\cdots FH$, $H_2O\cdots H_2O$, and $H_2O\cdots CFH_3$. In this way, hydrogen bonds where the strength is different are considered for systems that have been widely studied.[8,15,19−38] In section II the methodology used in this work is described, and in section III the results and discussion are presented. Finally, in section IV some conclusions are pointed out.

* Author to whom correspondence should be addressed. E-mail: jgo@xanum.uam.mx.

10.1021/jp046492+ CCC: $30.25
Published on Web 01/08/2005

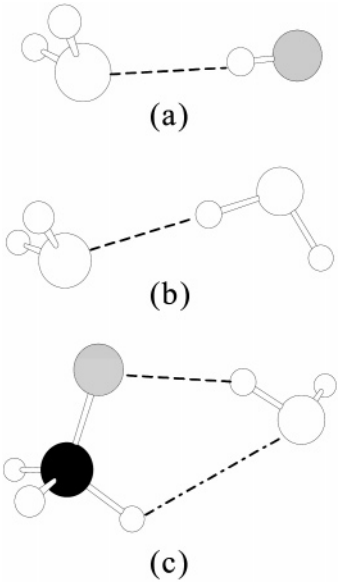

Figure 1. Optimized geometries with the MP2/aug-cc-pVTZ method. (a) $H_2O\cdots FH$, (b) $H_2O\cdots H_2O$, and (c) $H_2O\cdots CFH_3$.

TABLE 1: Hydrogen Bond Lengths, Distances between the Acceptor and the Donor, and Hydrogen Bond Angles[a]

	cc-pVTZ			
	MP2	B3LYP	BLYP	HF
		$H_2O\cdots FH$		
H−O···H−F	1.700	1.702 (0.1)	1.712 (0.7)	1.803 (6.1)
H−O···F−H	2.633	2.641 (0.3)	2.663 (1.1)	2.711 (3.0)
O−H−F	177.0	175.7	175.0	177.7
		$H_2O\cdots H_2O$		
H−O···H−O	1.930	1.958 (1.5)	1.977 (2.4)	2.094 (8.5)
H−O···O−H	2.894	2.926 (1.1)	2.956 (2.1)	3.038 (5.0)
O−H−O	179.3	179.4	179.1	179.9
		$H_2O\cdots CFH_3$		
C−F···H−O	1.986	2.036 (2.5)	2.056 (3.5)	2.166 (9.1)
C−F···O−H	2.872	2.914 (1.5)	2.947 (2.6)	3.012 (4.9)
F−H−O	152.2	150.4	151.1	148.9
H−O···H−C	2.637	2.730 (3.5)	2.753 (4.4)	2.940 (11.5)
H−O···C−H	3.258	3.339 (2.5)	3.372 (3.5)	3.503 (7.5)
O−H−C	116.0	115.0	115.5	112.8
	aug-cc-pVTZ			
	MP2	B3LYP	BLYP	HF
		$H_2O\cdots FH$		
H−O···H−F	1.678	1.694 (1.0)	1.702 (1.4)	1.806 (7.6)
H−O···F−H	2.617	2.637 (0.8)	2.659 (1.6)	2.716 (3.8)
O−H−F	178.2	177.7	177.7	178.3
		$H_2O\cdots H_2O$		
H−O···H−O	1.895	1.950 (2.9)	1.975 (4.2)	2.098 (10.7)
H−O···O−H	2.860	2.915 (1.9)	2.949 (3.1)	3.042
O−H−O	176.8	173.4	172.6	176.7
		$H_2O\cdots CFH_3$		
C−F···H−O	1.938	2.003 (3.4)	2.018 (4.1)	2.147 (10.8)
C−F···O−H	2.816	2.899 (2.9)	2.949 (4.7)	3.012 (7.0)
F−H−O	150.3	153.6	158.7	151.9
H−O···H−C	2.585	2.910 (12.6)	3.110 (20.3)	3.083 (19.3)
H−O···C−H	3.202	3.437 (7.3)	3.583 (11.9)	3.588 (12.1)
O−H−C	115.4	109.9	106.8	109.3

[a] All distances are in angstroms and angles are in degrees. Relative percent errors with respect to the MP2 method are in parentheses.

II. Methodology

The families of basis sets cc-pVXZ and aug-cc-pVXZ (with X = D, T, Q)[39] are used with the HF, KS, and MP2 methods. The exchange−correlation functionals tested for KS calculations were BLYP[40] and B3LYP;[41] thus, the generalized gradient approximation (GGA) is considered as well as a hybrid approach. A fine grid was used in the evaluation of the exchange−correlation contribution. One conformer for each system ($H_2O\cdots FH$, $H_2O\cdots H_2O$, and $H_2O\cdots CFH_3$) was studied and optimized by each method with the cc-pVTZ and aug-cc-pVTZ basis sets. Single point calculations with the cc-pVXZ at the optimized geometry with cc-pVTZ were carried out, and the same was carried out with the aug-cc-pVXZ basis sets at the aug-cc-pVTZ optimized geometry. The total energy for each conformer and each monomer is extrapolated to the CBS by using a mixed Gaussian exponential extrapolation approach.[42] The frequency analysis was performed with the B3LYP/cc-pVTZ method for each structure. All calculations were done with the NWChem v4.5 program.[43]

TABLE 2: Binding Energies for the $H_2O\cdots FH$, $H_2O\cdots H_2O$, and $H_2O\cdots CFH_3$ Systems, with BSSE (w/BSSE) and without it (w/o BSSE)[a]

	$H_2O\cdots FH$		$H_2O\cdots H_2O$		$H_2O\cdots CFH_3$	
method	w/o BSSE	w/ BSSE	w/o BSSE	w/ BSSE	w/o BSSE	w/ BSSE
MP2/cc-pVDZ	−11.6	−7.1	−7.4	−4.3	−6.2	−2.0
MP2/cc-pVTZ	−10.0	−7.9	−6.2	−4.8	−4.9	−2.9
MP2/cc-pVQZ	−9.5	−8.3	−5.6	−5.0	−4.2	−3.4
extrapolated	−9.1		−5.3		−3.8	
MP2/aug-cc-pVDZ	−9.3	−7.7	−5.4	−4.3	−4.7	−3.5
MP2/aug-cc-pVTZ	−10.1	−8.3	−6.3	−4.7	−5.2	−3.7
MP2/aug-cc-pVQZ	−10.1	−8.6	−5.8	−4.8	−4.3	−3.8
extrapolated	−10.0		−5.5		−3.8	
B3LYP/cc-pVDZ	−12.7	−8.5	−8.0	−4.5	−6.6	−2.4
B3LYP/cc-pVTZ	−10.2	−8.6	−5.8	−4.4	−4.2	−2.6
B3LYP/cc-pVQZ	−9.4	−8.7	−5.1	−4.5	−3.4	−2.7
extrapolated	−8.9		−4.6		−2.9	
B3LYP/aug-cc-pVDZ	−8.9	−8.7	−4.6	−4.5	−3.2	−3.0
B3LYP/aug-cc-pVTZ	−8.9	−8.8	−4.6	−4.5	−3.0	−3.0
B3LYP/aug-cc-pVQZ	−8.8	−8.8	−4.6	−4.5	−3.0	−3.0
extrapolated	−8.7		−4.5		−3.0	
BLYP/cc-pVDZ	−13.0	−8.0	−8.3	−4.1	−6.9	−2.0
BLYP/cc-pVTZ	−10.1	−8.1	−5.8	−4.0	−4.2	−2.2
BLYP/cc-pVQZ	−9.1	−8.3	−4.9	−4.0	−3.2	−2.3
extrapolated	−8.6		−4.3		−2.5	
BLYP/aug-cc-pVDZ	−8.5	−8.3	−4.2	−4.1	−2.8	−2.6
BLYP/aug-cc-pVTZ	−8.5	−8.4	−4.3	−4.1	−2.7	−2.6
BLYP/aug-cc-pVQZ	−8.4	−8.4	−4.2	−4.2	−2.7	−2.6
extrapolated	−8.3		−4.1		−2.6	
HF/cc-pVDZ	−9.6	−7.5	−5.7	−4.0	−4.3	−2.4
HF/cc-pVTZ	−8.0	−7.2	−4.4	−3.7	−3.0	−2.3
HF/cc-pVQZ	−7.5	−7.2	−3.9	−3.7	−2.6	−2.4
extrapolated	−7.2		−3.7		−2.3	
HF/aug-cc-pVDZ	−7.3	−7.1	−3.8	−3.7	−2.8	−2.6
HF/aug-cc-pVTZ	−7.2	−7.2	−3.7	−3.7	−2.5	−2.5
HF/aug-cc-pVQZ	−7.2	−7.2	−3.7	−3.7	−2.5	−2.5
extrapolated	−7.2		−3.7		−2.5	

[a] All quantities are in kcal/mol.

III. Results and Discussion

IIIa. Geometrical Parameters. The three studied conformers are depicted in Figure 1; no imaginary frequencies were found for these geometries. As we mentioned in the previous section, just one conformer was considered for each adduct, for example, in the case of the $H_2O\cdots FH$ system just the O···H contact was considered and not the F···H. Additionally, as we can see from Figure 1c that the $H_2O\cdots CFH_3$ adduct presents two hydrogen bond contacts. One of these contacts is a C−H···O hydrogen bond, which is well-known as a weak interaction.[34,44−48]

The hydrogen bond distances for each adduct are reported in Table 1. From this table it is clear that the MP2 method gives

TABLE 3: Energy Eigenvalues Obtained with the HF Method at the MP2/cc-pVTZ and MP2/aug-cc-pVTZ Geometries for the $H_2O\cdots FH$ System

	HOMO−3			HOMO		
	ϵ_{NG} (hartree)	ϵ_G (hartree)	$\lvert\epsilon_{NG}-\epsilon_G\rvert$ (kcal/mol)	ϵ_{NG} (hartree)	ϵ_G (hartree)	$\lvert\epsilon_{NG}-\epsilon_G\rvert$ (kcal/mol)
			H_2O			
cc-pVDZ	−1.3357	−1.3414	3.5	−0.4933	−0.4984	3.2
cc-pVTZ	−1.3453	−1.3476	1.4	−0.5051	−0.5070	1.2
cc-pVQZ	−1.3489	−1.3499	0.6	−0.5084	−0.5091	0.4
aug-cc-pVDZ	−1.3544	−1.3542	0.1	−0.5086	−0.5086	0.0
aug-cc-pVTZ	−1.3508	−1.3509	0.0	−0.5098	−0.5099	0.0
aug-cc-pVQZ	−1.3504	−1.3504	0.0	−0.5100	−0.5100	0.0
			FH			
cc-pVDZ	−1.5779	−1.5792	0.8	−0.6276	−0.6290	0.9
cc-pVTZ	−1.5893	−1.5901	0.5	−0.6424	−0.6431	0.5
cc-pVQZ	−1.5930	−1.5934	0.2	−0.6466	−0.6469	0.2
aug-cc-pVDZ	−1.6000	−1.6000	0.0	−0.6479	−0.6479	0.0
aug-cc-pVTZ	−1.5943	−1.5943	0.0	−0.6479	−0.6480	0.0
aug-cc-pVQZ	−1.5933	−1.5933	0.0	−0.6479	−0.6480	0.0
	LUMO			LUMO+3		
	ϵ_{NG} (hartree)	ϵ_G (hartree)	$\lvert\epsilon_{NG}-\epsilon_G\rvert$ (kcal/mol)	ϵ_{NG} (hartree)	ϵ_G (hartree)	$\lvert\epsilon_{NG}-\epsilon_G\rvert$ (kcal/mol)
			H_2O			
cc-pVDZ	0.1831	0.1760	4.4	0.8513	0.7315	75.2
cc-pVTZ	0.1321	0.1277	2.7	0.5697	0.5086	38.4
cc-pVQZ	0.1048	0.1018	1.9	0.4413	0.3930	30.3
aug-cc-pVDZ	0.0354	0.0342	0.8	0.1968	0.1579	24.4
aug-cc-pVTZ	0.0293	0.0280	0.8	0.1547	0.1171	23.6
aug-cc-pVQZ	0.0257	0.0248	0.6	0.1259	0.0953	19.3
			FH			
cc-pVDZ	0.1784	0.0962	51.6	1.4059	0.5520	535.8
cc-pVTZ	0.1303	0.0741	35.2	0.8240	0.3743	282.2
cc-pVQZ	0.1042	0.0613	27.0	0.5558	0.2879	168.1
aug-cc-pVDZ	0.0349	0.0229	7.5	0.2449	0.1262	74.5
aug-cc-pVTZ	0.0292	0.0192	6.3	0.1950	0.0975	61.2
aug-cc-pVQZ	0.0256	0.0173	5.2	0.1590	0.0806	49.2

TABLE 4: Energy Eigenvalues Obtained with the Exchange−Correlation Functional BLYP at the MP2/cc-pVTZ and MP2/aug-cc-pVTZ Geometries for the $H_2O\cdots FH$ System

	HOMO−3			HOMO		
	ϵ_{NG} (hartree)	ϵ_G (hartree)	$\lvert\epsilon_{NG}-\epsilon_G\rvert$ (kcal/mol)	ϵ_{NG} (hartree)	ϵ_G (hartree)	$\lvert\epsilon_{NG}-\epsilon_G\rvert$ (kcal/mol)
			H_2O			
cc-pVDZ	−0.8950	−0.9055	6.6	−0.2212	−0.2331	7.5
cc-pVTZ	−0.9130	−0.9175	2.8	−0.2485	−0.2536	3.2
cc-pVQZ	−0.9195	−0.9218	1.4	−0.2573	−0.2598	1.6
aug-cc-pVDZ	−0.9284	−0.9284	0.0	−0.2637	−0.2637	0.0
aug-cc-pVTZ	−0.9257	−0.9256	0.0	−0.2647	−0.2647	0.0
aug-cc-pVQZ	−0.9252	−0.9251	0.0	−0.2648	−0.2648	0.0
			FH			
cc-pVDZ	−1.0527	−1.0554	1.7	−0.3006	−0.3035	1.9
cc-pVTZ	−1.0787	−1.0807	1.2	−0.3344	−0.3364	1.3
cc-pVQZ	−1.0874	−1.0886	0.7	−0.3450	−0.3462	0.8
aug-cc-pVDZ	−1.0980	−1.0980	0.0	−0.3516	−0.3516	0.0
aug-cc-pVTZ	−1.0939	−1.0939	0.0	−0.3523	−0.3523	0.0
aug-cc-pVQZ	−1.0931	−1.0931	0.0	−0.3524	−0.3524	0.0
	LUMO			LUMO+3		
	ϵ_{NG} (hartree)	ϵ_G (hartree)	$\lvert\epsilon_{NG}-\epsilon_G\rvert$ (kcal/mol)	ϵ_{NG} (hartree)	ϵ_G (hartree)	$\lvert\epsilon_{NG}-\epsilon_G\rvert$ (kcal/mol)
			H_2O			
cc-pVDZ	0.0261	0.0202	3.7	0.5647	0.5078	35.8
cc-pVTZ	−0.0018	−0.0047	1.8	0.3594	0.3150	27.9
cc-pVQZ	−0.0148	−0.0165	1.1	0.2784	0.2475	19.4
aug-cc-pVDZ	−0.0391	−0.0393	0.1	0.1043	0.0814	14.4
aug-cc-pVTZ	−0.0393	−0.0393	0.0	0.0811	0.0590	13.9
aug-cc-pVQZ	−0.0393	−0.0393	0.0	0.0651	0.0476	11.0
			FH			
cc-pVDZ	0.0179	−0.0065	15.3	1.0505	0.4332	387.4
cc-pVTZ	−0.0091	−0.0229	8.6	0.5878	0.2566	207.9
cc-pVQZ	−0.0216	−0.0306	5.7	0.3742	0.1906	115.2
aug-cc-pVDZ	−0.0452	−0.0451	0.1	0.1353	0.0572	49.0
aug-cc-pVTZ	−0.0450	−0.0446	0.2	0.1058	0.0459	37.6
aug-cc-pVQZ	−0.0448	−0.0447	0.1	0.0855	0.0398	28.7

TABLE 5: Energy Eigenvalues Obtained with the Exchange−Correlation Functional B3LYP at the MP2/cc-pVTZ and MP2/aug-cc-pVTZ Geometries for the $H_2O\cdots FH$ System

	HOMO−3			HOMO		
	ϵ_{NG} (hartree)	ϵ_G (hartree)	$\lvert\epsilon_{NG} - \epsilon_G\rvert$ (kcal/mol)	ϵ_{NG} (hartree)	ϵ_G (hartree)	$\lvert\epsilon_{NG} - \epsilon_G\rvert$ (kcal/mol)
			H_2O			
cc-pVDZ	−0.9950	−1.0040	5.6	−0.2885	−0.2983	6.1
cc-pVTZ	−1.0108	−1.0146	2.4	−0.3117	−0.3157	2.5
cc-pVQZ	−1.0165	−1.0183	1.1	−0.3189	−0.3208	1.2
aug-cc-pVDZ	−1.0241	−1.0241	0.0	−0.3231	−0.3231	0.0
aug-cc-pVTZ	−1.0211	−1.0211	0.0	−0.3241	−0.3242	0.0
aug-cc-pVQZ	−1.0207	−1.0206	0.0	−0.3243	−0.3243	0.0
			FH			
cc-pVDZ	−1.1700	−1.1722	1.4	−0.3797	−0.3822	1.6
cc-pVTZ	−1.1922	−1.1938	1.0	−0.4085	−0.4101	1.0
cc-pVQZ	−1.1994	−1.2003	0.6	−0.4172	−0.4181	0.6
aug-cc-pVDZ	−1.2086	−1.2087	0.1	−0.4217	−0.4218	0.0
aug-cc-pVTZ	−1.2041	−1.2041	0.0	−0.4223	−0.4223	0.0
aug-cc-pVQZ	−1.2033	−1.2033	0.0	−0.4224	−0.4224	0.0
	LUMO			LUMO+3		
	ϵ_{NG} (hartree)	ϵ_G (hartree)	$\lvert\epsilon_{NG} - \epsilon_G\rvert$ (kcal/mol)	ϵ_{NG} (hartree)	ϵ_G (hartree)	$\lvert\epsilon_{NG} - \epsilon_G\rvert$ (kcal/mol)
			H_2O			
cc-pVDZ	0.0500	0.0441	3.8	0.6117	0.5516	37.7
cc-pVTZ	0.0192	0.0164	1.8	0.3926	0.3454	29.6
cc-pVQZ	0.0046	0.0028	1.1	0.3054	0.2730	20.3
aug-cc-pVDZ	−0.0246	−0.0248	0.1	0.1188	0.0941	15.5
aug-cc-pVTZ	−0.0252	−0.0253	0.0	0.0931	0.0690	15.1
aug-cc-pVQZ	−0.0254	−0.0255	0.0	0.0755	0.0563	12.0
			FH			
cc-pVDZ	0.0431	0.0130	18.9	1.1089	0.4591	407.8
cc-pVTZ	0.0137	−0.0039	11.0	0.6247	0.2793	216.7
cc-pVQZ	−0.0003	−0.0012	0.6	0.4019	0.2107	120.0
aug-cc-pVDZ	−0.0288	−0.0291	0.1	0.1527	0.0698	52.0
aug-cc-pVTZ	−0.0290	−0.0288	0.1	0.1203	0.0569	39.8
aug-cc-pVQZ	−0.0289	−0.0290	0.0	0.0979	0.0496	30.3

TABLE 6: Energy Eigenvalues Obtained with the HF Method at the MP2/cc-pVTZ and MP2/aug-cc-pVTZ Geometries for the $H_2O\cdots CFH_3$ System

	HOMO−3			HOMO		
	ϵ_{NG} (hartree)	ϵ_G (hartree)	$\lvert\epsilon_{NG} - \epsilon_G\rvert$ (kcal/mol)	ϵ_{NG} (hartree)	ϵ_G (hartree)	$\lvert\epsilon_{NG} - \epsilon_G\rvert$ (kcal/mol)
			H_2O			
cc-pVDZ	−1.3366	−1.3399	2.1	−0.4937	−0.4959	1.4
cc-pVTZ	−1.3461	−1.3480	1.2	−0.5054	−0.5066	0.7
cc-pVQZ	−1.3497	−1.3506	0.6	−0.5087	−0.5092	0.3
aug-cc-pVDZ	−1.3545	−1.3545	0.0	−0.5087	−0.5086	0.1
aug-cc-pVTZ	−1.3510	−1.3510	0.0	−0.5099	−0.5099	0.0
aug-cc-pVQZ	−1.3505	−1.3505	0.0	−0.5100	−0.5100	0.0
			CFH_3			
cc-pVDZ	−0.6854	−0.6878	1.5	−0.5248	−0.5284	2.2
cc-pVTZ	−0.6916	−0.6926	0.6	−0.5295	−0.5321	1.6
cc-pVQZ	−0.6937	−0.6940	0.2	−0.5313	−0.5334	1.3
aug-cc-pVDZ	−0.6935	−0.6934	0.1	−0.5334	−0.5333	0.1
aug-cc-pVTZ	−0.6934	−0.6934	0.0	−0.5341	−0.5340	0.0
aug-cc-pVQZ	−0.6935	−0.6935	0.0	−0.5342	−0.5342	0.0
	LUMO			LUMO+3		
	ϵ_{NG} (hartree)	ϵ_G (hartree)	$\lvert\epsilon_{NG} - \epsilon_G\rvert$ (kcal/mol)	ϵ_{NG} (hartree)	ϵ_G (hartree)	$\lvert\epsilon_{NG} - \epsilon_G\rvert$ (kcal/mol)
			H_2O			
cc-pVDZ	0.1829	0.1102	45.6	0.8560	0.2478	381.7
cc-pVTZ	0.1319	0.0840	30.0	0.5729	0.1951	273.1
cc-pVQZ	0.1046	0.0687	22.5	0.4417	0.1627	175.1
aug-cc-pVDZ	0.0354	0.0264	5.6	0.1968	0.0653	82.5
aug-cc-pVTZ	0.0293	0.0217	4.8	0.1547	0.0532	63.7
aug-cc-pVQZ	0.0257	0.0189	4.3	0.1259	0.0477	49.1
			CFH_3			
cc-pVDZ	0.1884	0.1483	25.2	0.2897	0.2660	14.8
cc-pVTZ	0.1377	0.1144	14.6	0.2266	0.2143	7.7
cc-pVQZ	0.1108	0.0941	10.4	0.1851	0.1782	4.3
aug-cc-pVDZ	0.0339	0.0321	1.1	0.0870	0.0621	15.6
aug-cc-pVTZ	0.0275	0.0260	1.0	0.0736	0.0500	14.8
aug-cc-pVQZ	0.0228	0.0222	0.3	0.0632	0.0450	11.4

TABLE 7: Energy Eigenvalues Obtained with the Exchange−Correlation Functional BLYP at the MP2/cc-pVTZ and MP2/aug-cc-pVTZ Geometries for the $H_2O\cdots CFH_3$ System

	HOMO−3			HOMO		
	ϵ_{NG} (hartree)	ϵ_G (hartree)	$\lvert\epsilon_{NG}-\epsilon_G\rvert$ (kcal/mol)	ϵ_{NG} (hartree)	ϵ_G (hartree)	$\lvert\epsilon_{NG}-\epsilon_G\rvert$ (kcal/mol)
			H_2O			
cc-pVDZ	−0.8959	−0.9021	3.9	−0.2215	−0.2296	5.0
cc-pVTZ	−0.9138	−0.9176	2.4	−0.2487	−0.2533	2.9
cc-pVQZ	−0.9203	−0.9225	1.4	−0.2575	−0.2601	1.7
aug-cc-pVDZ	−0.9285	−0.9285	0.0	−0.2637	−0.2636	0.1
aug-cc-pVTZ	−0.9258	−0.9258	0.0	−0.2647	−0.2647	0.0
aug-cc-pVQZ	−0.9253	−0.9253	0.0	−0.2648	−0.2648	0.0
			CFH_3			
cc-pVDZ	−0.4104	−0.4140	2.3	−0.2688	−0.2740	3.3
cc-pVTZ	−0.4220	−0.4235	1.0	−0.2871	−0.2891	1.3
cc-pVQZ	−0.4251	−0.4258	0.4	−0.2921	−0.2930	0.6
aug-cc-pVDZ	−0.4258	−0.4258	0.0	−0.2939	−0.2939	0.0
aug-cc-pVTZ	−0.4263	−0.4263	0.0	−0.2950	−0.2950	0.0
aug-cc-pVQZ	−0.4264	−0.4264	0.0	−0.2951	−0.2952	0.0
	LUMO			LUMO+3		
	ϵ_{NG} (hartree)	ϵ_G (hartree)	$\lvert\epsilon_{NG}-\epsilon_G\rvert$ (kcal/mol)	ϵ_{NG} (hartree)	ϵ_G (hartree)	$\lvert\epsilon_{NG}-\epsilon_G\rvert$ (kcal/mol)
			H_2O			
cc-pVDZ	0.0259	0.0134	7.9	0.5685	0.2058	227.6
cc-pVTZ	−0.0020	−0.0096	4.8	0.3622	0.1616	125.9
cc-pVQZ	−0.0149	−0.0203	3.3	0.2806	0.1330	92.6
aug-cc-pVDZ	−0.0391	−0.0392	0.0	0.1043	0.0461	36.5
aug-cc-pVTZ	−0.0392	−0.0393	0.0	0.0811	0.0365	28.0
aug-cc-pVQZ	−0.0393	−0.0394	0.1	0.0651	0.0328	20.3
			CFH_3			
cc-pVDZ	0.0498	0.0419	4.9	0.1097	0.1080	1.0
cc-pVTZ	0.0232	0.0181	3.2	0.0861	0.0855	0.3
cc-pVQZ	0.0104	0.0068	2.3	0.0717	0.0714	0.2
aug-cc-pVDZ	−0.0186	−0.0186	0.0	0.0172	0.0170	0.1
aug-cc-pVTZ	−0.0192	−0.0193	0.0	0.0140	0.0138	0.1
aug-cc-pVQZ	−0.0198	−0.0198	0.0	0.0123	0.0122	0.1

TABLE 8: Energy Eigenvalues Obtained with the Exchange−Correlation Functional B3LYP at the MP2/cc-pVTZ and MP2/aug-cc-pVTZ Geometries for the $H_2O\cdots CFH_3$ System

	HOMO−3			HOMO		
	ϵ_{NG} (hartree)	ϵ_G (hartree)	$\lvert\epsilon_{NG}-\epsilon_G\rvert$ (kcal/mol)	ϵ_{NG} (hartree)	ϵ_G (hartree)	$\lvert\epsilon_{NG}-\epsilon_G\rvert$ (kcal/mol)
			H_2O			
cc-pVDZ	−0.9958	−1.0011	3.3	−0.2888	−0.2950	3.9
cc-pVTZ	−1.0116	−1.0147	2.0	−0.3120	−0.3154	2.1
cc-pVQZ	−1.0172	−1.0190	1.1	−0.3191	−0.3210	1.2
aug-cc-pVDZ	−1.0243	−1.0242	0.0	−0.3231	−0.3231	0.0
aug-cc-pVTZ	−1.0213	−1.0212	0.0	−0.3242	−0.3242	0.0
aug-cc-pVQZ	−1.0208	−1.0208	0.0	−0.3243	−0.3243	0.0
			CFH_3			
cc-pVDZ	−0.4748	−0.4783	2.2	−0.3348	−0.3392	2.8
cc-pVTZ	−0.4857	−0.4870	0.8	−0.3495	−0.3511	1.0
cc-pVQZ	−0.4886	−0.4891	0.4	−0.3535	−0.3542	0.4
aug-cc-pVDZ	−0.4888	−0.4888	0.0	−0.3545	−0.3545	0.0
aug-cc-pVTZ	−0.4892	−0.4892	0.0	−0.3555	−0.3555	0.0
aug-cc-pVQZ	−0.4893	−0.4893	0.0	−0.3557	−0.3557	0.0
	LUMO			LUMO+3		
	ϵ_{NG} (hartree)	ϵ_G (hartree)	$\lvert\epsilon_{NG}-\epsilon_G\rvert$ (kcal/mol)	ϵ_{NG} (hartree)	ϵ_G (hartree)	$\lvert\epsilon_{NG}-\epsilon_G\rvert$ (kcal/mol)
			H_2O			
cc-pVDZ	0.0498	0.0341	9.9	0.6157	0.2167	250.3
cc-pVTZ	0.0190	0.0095	6.0	0.3956	0.1705	141.3
cc-pVQZ	0.0044	−0.0024	4.2	0.3075	0.1400	105.1
aug-cc-pVDZ	−0.0246	−0.0249	0.2	0.1188	0.0489	43.9
aug-cc-pVTZ	−0.0252	−0.0254	0.1	0.0931	0.0393	33.8
aug-cc-pVQZ	−0.0254	−0.0256	0.1	0.0755	0.0366	24.4
			CFH_3			
cc-pVDZ	0.0699	0.0610	5.6	0.1316	0.1302	0.9
cc-pVTZ	0.0404	0.0348	3.5	0.1054	0.1049	0.3
cc-pVQZ	0.0260	0.0220	2.6	0.0888	0.0885	0.2
aug-cc-pVDZ	−0.0086	−0.0087	0.1	0.0249	0.0246	0.2
aug-cc-pVTZ	−0.0096	−0.0097	0.1	0.0209	0.0206	0.2
aug-cc-pVQZ	−0.0102	−0.0103	0.1	0.0198	0.0195	0.2

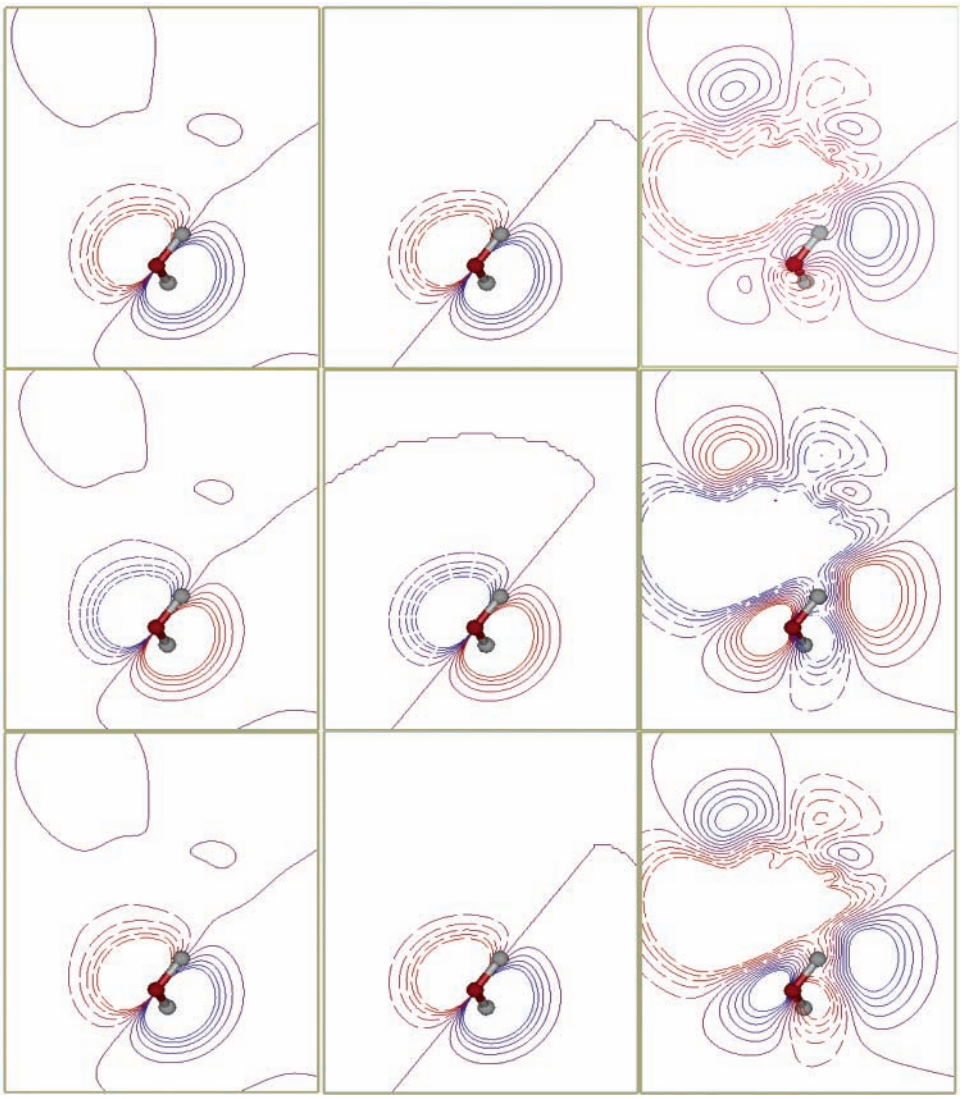

Figure 2. Contour map of the HOMO obtained with HF, BLYP, and B3LYP methods with the cc-pVDZ basis set. $\psi_G(\mathbf{r})$ is in the first column, $\psi_{NG}(\mathbf{r})$ is in the second, and $\psi_G(\mathbf{r}) - \psi_{NG}(\mathbf{r})$ is in the third column. The HF results are in the first row, those corresponding to BLYP are in the second row, and in the third row the B3LYP results are presented. See details in the text. Dotted lines correspond to negative values.

the shortest distances independently of the system considered and the basis set used. We must take into account that the potential energy surface considered in this work is not corrected by the BSSE; it is known that the hydrogen bond lengths are shorter if this correction is not considered.[8] If we use the MP2 method as a reference, it is evident that the HF method gives the largest deviations and the B3LYP method gives the most similar results, suggesting that the correlation contribution is important for geometrical parameters in this kind of system. It is worth noting that, in the $H_2O\cdots CFH_3$ adduct, where the weak interaction H−O···H−C is present, the differences between the methods in the geometry parameters are more pronounced. The presence of diffuse functions, in almost all systems, shrinks the bond length of the hydrogen bond for the methods that incorporate correlation contributions. The HF method does not show such a trend. Except for the H−O···H−C contact where this behavior is preserved just for the MP2 method, because the KS results behave as the HF approach.

IIIb. Strength of the Hydrogen Bond. The binding energies for adducts are reported in Table 2. The strength of the hydrogen bond is estimated with the BSSE correction and without it. Additionally, CBS values for the binding energies are also reported. As it is expected, from this table the strongest hydrogen bond is found in the $H_2O\cdots FH$ adduct, and the weakest in the $H_2O\cdots CFH_3$. These results are in agreement with the distances reported in Table 1, where the shortest contact is presented in the $H_2O\cdots FH$ system and the largest is in $H_2O\cdots CFH_3$. A lot of information can be extracted from Table 2. First, independently of the basis set considered, HF, BLYP, and B3LYP binding energies with the BSSE correction included are almost the same when they are compared within each method. This observation is not true for MP2, because in this method the BSSE is overestimated for the smallest basis set and consequently the binding energy is underestimated.

Second, if we use as a reference the CBS binding energies, in absolute value, it is clear that for the MP2 method the extrapolated values represent an upper bound over those obtained with the BSSE correction. It is important to note that HF, BLYP, and B3LYP methods give similar results between the extrapolated approach and the BSSE-corrected method. In particular, when diffuse functions are used the binding energies with or without BSSE are practically the same as that obtained with the extrapolated technique. For the MP2 method, a contrary behavior is obtained because, even when a large basis set is used, there are some discrepancies between the extrapolated and the BSSE-corrected values, particularly for the $H_2O\cdots FH$ system. Third, the HF method gives the smallest BSSE followed by the B3LYP, BLYP, and MP2 methods. This ordering is not

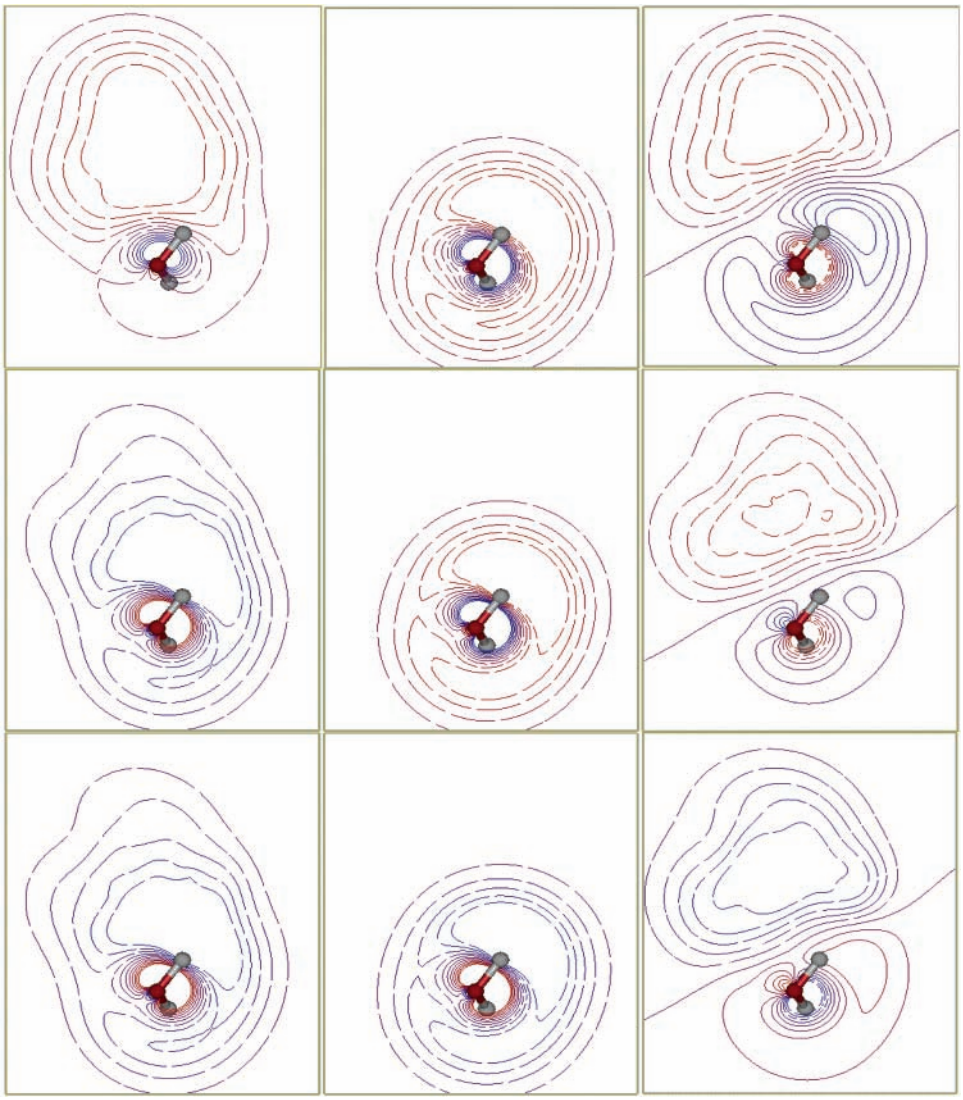

Figure 3. Contour map of the LUMO obtained with the HF, BLYP, and B3LYP methods with the cc-pVDZ basis set. $\psi_G(\mathbf{r})$ is in the first column, $\psi_{NG}(\mathbf{r})$ is in the second, and $\psi_G(\mathbf{r}) - \psi_{NG}(\mathbf{r})$ is in the third column. The HF results are in the first row, those corresponding to BLYP are in the second row, and in the third row the B3LYP results are presented. See details in the text. Dotted lines correspond to negative values.

true when the cc-pVDZ basis set is used, because the BLYP and MP2 give similar results. This behavior is a consequence of the cc-pVDZ basis set deficiencies.

Fourth, with respect to CBS binding energies, the MP2 method predicts stronger hydrogen bonds for any system, with or without BSSE correction. This result is consistent with the shorter distances obtained for this method and reported in Table 1. However, these CBS binding energies were obtained on noncorrected geometries, and it is expected that if the BSSE is removed in the optimization process, longer contact distances can be obtained and consequently weaker binding energies can be found.[8] Fifth, the diffuse functions give a stronger binding energy with the MP2 method. That is not true for the others methods, in fact the KS and HF methods are nonsensitive to these kind of functions when the BSSE is corrected.

IIIc. BSSE on the Orbital Energies. From the analysis of the previous paragraph, clearly the MP2 method does not follow the same trend as the HF or KS methods. As we mentioned before, the main difference between MP2 and the other methods considered in this work is that this methodology uses virtual orbitals to compute the total energy. Thus, it is interesting to see how the BSSE modifies occupied and unoccupied orbital energies. In Tables 3−5 we are reporting the HF, BLYP, and B3LYP occupied and unoccupied orbital energies, respectively, for the monomers H_2O and FH at the geometry of the system with the strongest hydrogen bond ($H_2O\cdots FH$). Additionally, in Tables 6−8 the same quantities are reported for the monomers H_2O and CFH_3 at the geometry of the system with the weakest hydrogen bond ($H_2O\cdots CFH_3$). In all of these tables two occupied orbital energies are included, the HOMO and the orbital three places below it (HOMO−3). Also two unoccupied orbital energies are reported, the LUMO and the orbital three places above of it (LUMO+3). The selection of the HOMO−3 and LUMO+3 was arbitrary, just to show some examples beyond the HOMO and LUMO. Each orbital energy was obtained with the basis set of the monomer and with the additional "ghost" basis set provided by the other monomer; in this sense we have an orbital energy without a "ghost" (ϵ_{NG}) and with a "ghost" (ϵ_G). The absolute difference between these orbital energies is also listed in these tables.

We see in Table 3, where the HF orbital energies are shown, that for the same basis set the orbital energies ϵ_{NG} and ϵ_G present almost the same differences for the occupied orbitals. The biggest difference is found when the smallest basis set is used. The FH monomer presents a smaller difference between ϵ_{NG} and ϵ_G with respect to H_2O. It is clear that the diffuse functions

stabilize the occupied HF orbitals and give the same orbital energies with or without "ghost" basis sets. For the unoccupied HF orbitals it is found that diffuse functions reduce the orbital energy difference drastically. However, clearly the unoccupied HF orbital energies are quite different if "ghost" basis sets are present or not. This result will have a big impact in the MP2 energy because this method is based on occupied and unoccupied HF orbitals. Thus, if the BSSE is relevant on the unoccupied HF orbitals, then it will be important in the calculation of the MP2 total energy. In particular for the LUMO+3 orbital in the FH monomer the aug-cc-pVQZ gives 49.2 kcal/mol as a difference between ϵ_{NG} and ϵ_G, which is a big difference considering the basis set used. We can see in Table 3 that the occupied HF orbital energies are almost converged when diffuse functions are used, but that is not true for the unoccupied orbital energies because they exhibit large changes when the basis set is changed.

In Table 4 the same information as in Table 3 is presented, except that in Table 4 the BLYP method is used instead of the HF method. Comparing Tables 3 and 4 we see two facts that have been discussed previously in the literature:

(a) The occupied HF orbitals are deeper than the KS orbitals obtained with a GGA exchange−correlation functional.[4,5] It is well-known that the HF HOMO energy is a good approximation to the ionization potential for many systems, the discrepancies observed between Table 3 and Table 4 show that the HOMO energy obtained with BLYP method cannot be a good approximation to this property.[5] It is clear that the occupied BLYP orbitals, obtained with the cc-pVXZ basis sets, present a bigger difference between ϵ_{NG} and ϵ_G with respect to the HF results for the same system. When diffuse functions are used the BLYP occupied orbital energies are almost converged and do not present a difference when the "ghost" basis set is used; this fact has impact in the BSSE as it can be seen in Table 2 for the BLYP method with diffuse functions. Furthermore, we can see that with these basis sets the occupied orbital energies are almost converged.

(b) The unoccupied KS orbitals obtained with a GGA exchange−correlation functional are deeper than those obtained with the HF method. In fact, for our systems the BLYP LUMO energy is bound and that of the HF is not. In particular, convergence for the LUMO energy has been observed when the basis set is increased in some systems.[49] The physical meaning of the unoccupied orbital energies for HF and KS is still discussed, and it was explored systematically for ionic systems.[5]

In Table 5 the B3LYP orbital energies show a behavior between that of Table 3 and that of Table 4, and we must remember that the B3LYP exchange−correlation functional is built with a fraction of the HF exchange; thus, the B3LYP occupied orbital energies are lower than those obtained with BLYP and bigger than those obtained with HF. For the unoccupied orbital energies the behavior is different because the B3LYP gives bigger orbital energies than BLYP but lower orbital energies than HF.

In Tables 6 and 7 the same orbital energies obtained with HF and BLYP are presented for a system with a weaker hydrogen bond. Comparing these tables with Tables 3 and 4 we observe bigger differences between ϵ_{NG} and ϵ_G for the $H_2O\cdots CFH_3$ adduct than those obtained in systems where the hydrogen bond is stronger. In consequence the BSSE will be bigger in this system, as it is corroborated in Table 2. Curiously the unoccupied orbitals of the fragment CFH_3 is almost not sensitive to the "ghost" basis set provided by the H_2O. The same orbital energies obtained with the B3LYP method are reported in Table 8, where it is clear that this method gives results that fall between those of HF and those of BLYP.

IIId. BSSE on the Orbitals. It is reasonable to think that if the orbital energies are modified with the "ghost" basis sets their corresponding functions are as well. The HOMO and LUMO orbital functions with "ghost", $\psi_G(\mathbf{r})$, and no "ghost", $\psi_{NG}(\mathbf{r})$, functions are depicted in Figures 2 and 3, respectively. Also the difference $\psi_G(\mathbf{r}) - \psi_{NG}(\mathbf{r})$ is presented in these figures. All of these figures correspond to the water molecule in the $H_2O\cdots CFH_3$ adduct and the cc-pVDZ basis set, which is the worst basis set tested.

As we can see from these figures the "ghost" basis set, provided by the CFH_3, has an important impact in both orbital functions of the water. In particular, we can see more extended regions obtained by the HF method for the $\psi_G^{LUMO}(\mathbf{r})$ than the BLYP method. Thus, as in the orbital energies, the HF LUMO is more sensitive to the "ghost" basis set than that obtained with the BLYP method. Contrary to this behavior the difference $\psi_G^{HOMO}(\mathbf{r}) - \psi_{NG}^{HOMO}(\mathbf{r})$ obtained with the BLYP method covers more extended regions than that obtained with the HF method, indicating that the HF HOMO function is less sensitive than the BLYP HOMO with the presence of the "ghost" basis set. The same conclusions can be obtained with a large basis set, such as the aug-cc-pVQZ, but the difference $\psi_G(\mathbf{r}) - \psi_{NG}(\mathbf{r})$ is more pronounced with the cc-pVDZ basis set.

IV. Conclusions

In this work three systems with different hydrogen bond strengths were studied by using HF, KS, and MP2 methods. As it was found in other works, the BSSE is important to predict the binding energy in systems linked by hydrogen bonds. Besides, to reduce such error it is mandatory to use basis sets with diffuse functions in this kind of system. We also studied the impact of the BSSE on the HF and KS orbitals. From this study two important conclusions can be addressed:

(1) The occupied KS orbitals are more sensitive than the occupied HF orbitals to the presence of a "ghost" basis set. This observation strongly suggests that the binding energies predicted with HF have a minor contribution due to the BSSE than those obtained with the KS method. This conclusion is in accordance with the fact that the KS electron density, which is built using the KS orbitals, is more sensitive to the BSSE than that obtained with the HF method.[50]

(2) The unoccupied HF orbitals are more sensitive to the presence of a "ghost" basis set than its occupied orbitals and even the unoccupied KS orbitals. Because the MP2 method is based on the all HF orbitals, the expected BSSE will be greater than that obtained with the HF or KS method. It has been suggested that correlated methods work better with a local-multiplicative potential.[51] In this work we propose using these correlated methods with a local-multiplicative potential to obtain a lower BSSE.

Acknowledgment. Financial support for R.V. and J.-Z.R. was provided by CONACYT, México, through Project No. C01-39621 and the scholarship 169487, respectively. We thank the Laboratorio de Visualización y Cómputo Paralelo at UAM − Iztapalapa for the access to its computer facilities.

References and Notes

(1) (a) Møller, C.; Plesset, M. S. *Phys. Rev.* **1934**, *46*, 618. (b) Szabo, A.; Ostlund, N. S. *Modern Quantum Chemistry: Introduction to Advanced Electronic Structure Theory*, 1st ed.; McGraw-Hill: New York, 1989 (revised).

(2) (a) Kohn, W.; Sham, L. J. *Phys. Rev. A* **1965**, *140*, 1133. (b) Parr, R. G.; Yang, W. *Density-Functional Theory of Atoms and Molecules*; Oxford University Press: New York, 1989.

(3) Garza, J.; Nichols, J. A.; Dixon, D. A. *J. Chem. Phys.* **2000**, *113*, 6029.

(4) Aparicio, F.; Garza, J.; Cedillo, A.; Galván, M.; Vargas, R. In *Reviews of Modern Quantum Chemistry*; Sen, K. D., Ed.; World Scientific: Singapore, 2002; Vol. 1, p 755.

(5) Garza, J.; Fahlstrom, C. A.; Vargas, R.; Nichols, J. A.; Dixon, D. A. in *Reviews of Modern Quantum Chemistry*; Sen, K. D., Ed.; World Scientific: Singapore, 2002; Vol. 1, p 1508.

(6) Jansen, H. B.; Ross, P. *Chem. Phys. Lett.* **1969**, *3*, 140.

(7) Boys, S. B.; Bernardi, F. *Mol. Phys.* **1970**, *19*, 533.

(8) (a) Mayer, I.; Surjan, P. R. *Chem. Phys. Lett.* **1992**, *191*, 497. (b) Simon, S.; Duran, M.; Dannenberg, J. J. *J. Chem. Phys.* **1996**, *105*, 11024. (c) Salvador, P.; Paizs, B.; Duran, M.; Suhai, S. *J. Comput. Chem.* **2001**, *22*, 765.

(9) Mayer, I. *Int. J. Quantum Chem.* **1983**, *23*, 341.

(10) Mayer, I.; Vibók, Á. *Int. J. Quantum Chem.* **1991**, *15*, 139.

(11) Mayer, I.; Túri, L. *THEOCHEM* **1991**, *227*, 43.

(12) Lotrich, V. F.; Szalewicz, K. *J. Chem. Phys.* **2000**, *112*, 112.

(13) Gianinetti, E.; Vandoni, I.; Famulari, A.; Raimondi, M. *Adv. Quantum Chem.* **1999**, *31*, 251.

(14) Nagata, T.; Iwata, S. *J. Chem. Phys.* **2004**, *120*, 3555.

(15) Paizs, B.; Suhai, S. *J. Comput. Chem.* **1998**, *19*, 575.

(16) Valivon, P.; Vibók, Á.; Mayer, I. *J. Comput. Chem.* **1993**, *14*, 401.

(17) Kim, K.; Jordan, K. D. *J. Phys. Chem.* **1994**, *98*, 10089.

(18) Gu, Y.; Kar, T.; Scheiner, S. *J. Am. Chem. Soc.* **1999**, *121*, 9411.

(19) Tursi, A.; Nixon, E. R. *J. Chem. Phys.* **1970**, *52*, 1521.

(20) Dyke, T. R.; Mack, K. M.; Muenter, J. S. *J. Chem. Phys.* **1977**, *66*, 498.

(21) Fredin, L.; Nelander, B.; Ribbegard, G. *J. Chem. Phys.* **1977**, *66*, 4065.

(22) Wuelfert, S.; Herren, D.; Leutwyler, S. *J. Chem Phys.* **1987**, *86*, 3751.

(23) Curtis, L. A.; Frurip, D. J.; Blander, M. *J. Chem. Phys.* **1979**, *71*, 2703.

(24) Reimers, J.; Watts, R.; Klein, M. *Chem. Phys.* **1982**, *64*, 95.

(25) Odutola, J. A.; Dyke, T. R. *J. Chem. Phys.* **1980**, *72*, 5062.

(26) Ventura, O. N.; Irving, K.; Latajka, Z. *Chem. Phys. Lett*. **1994**, *217*, 436.

(27) Baum, J. O.; Finney, J. L. *Mol. Phys.* **1985**, *55*, 1097.

(28) Frisch, M. J.; Del Bene, J. E.; Binkley, J. S.; Schaeffer, H. F., III. *J. Chem. Phys.* **1986**, *84*, 2279.

(29) Del Bene, J. E.; Person, W. B.; Szczepaniak, K. *J. Phys. Chem*. **1995**, *99*, 10705.

(30) Frisch, M. J.; Pople, J. A.; Del Bene, J. E. *J. Phys. Chem.* **1985**, *89*, 3664.

(31) Sim, F.; St. Amant, A.; Papai, I.; Salahub, D. R. *J. Am. Chem. Soc.* **1992**, *114*, 4391.

(32) Feller, D. *J. Chem. Phys.* **1992**, *96*, 6104.

(33) (a) Xantheas, S. S.; Dunning, T. H., Jr. *J. Chem. Phys*. **1993**, *98*, 8037. (b) Xantheas, S. S.; Dunning, T. H., Jr. *J. Chem. Phys.* **1993**, *99*, 8774. (c) Xantheas, S. S. *J. Chem. Phys.* **1994**, *100*, 7523. (d) Xantheas, S. S. *J. Chem. Phys.* **1995**, *102*, 4505.

(34) Kryechko, E. S.; Zeegers-Huyskens, T. *J. Phys. Chem. A* **2001**, *105*, 7118.

(35) Alkorta, I.; Malvendes, S. *J. Phys. Chem*. **1995**, *99*, 6457.

(36) Novoa, J. J.; Sosa, C. *J. Phys. Chem.* **1994**, *99*, 15837.

(37) Hobza, P.; Šponer, J.; Reschel, T. *J. Comput. Chem.* **1995**, *16*, 1315.

(38) Legon, A. C.; Millen, D. J.; North, H. M. *Chem. Phys. Lett.* **1987**, *135*, 303.

(39) Dunning, T. H., Jr. *J. Chem. Phys.* **1989**, *90*, 1007.

(40) (a) Becke, A. D. *Phys. Rev. A* **1988**, *38*, 3098. (b) Lee, C.; Yang, W.; Parr, R. G. *Phys. Rev. B* **1988**, *37*, 78.

(41) (a) Becke, A. D. *J. Chem. Phys.* **1993**, *98*, 5648. (b) Becke, A. D. *J. Chem. Phys.* **1993**, *98*, 1372.

(42) Peterson, K. A.; Woon, D. E.; Dunning, T. H., Jr. *J. Chem. Phys.* **1994**, *100*, 7410.

(43) Bernholdt, D. E.; Apra, E.; Fruchtl, H. A.; Guest, M. F.; Harrison, R. J.; Kendall, R. A.; Dutteh, R. A.; Long, X.; Nicholas, J. B.; Nichols, J. A.; Taylor, H. L.; Wong, A. T.; Fann, G. I.; Littlefield, R. J.; Nieplocha, J. *Int. J. Quantum Chem., Quantum Chem. Symp.* **1995**, *29*, 475.

(44) Wang, B.; Hinton, J. F.; Pulay, P. *J. Phys. Chem. A* **2003**, *107*, 4683.

(45) Vargas, R.; Garza, J.; Dixon, D. A.; Hay, B. P. *J. Am. Chem. Soc.* **2000**, *122*, 4750.

(46) Scheiner, S.; Kar, T. *J. Phys. Chem. A* **2002**, *106*, 1784.

(47) Green, R. D. *Hydrogen Bonding by C-H Groups*; Wiley: New York, 1974.

(48) (a) Garza, J.; Vargas, R.; Gómez, M.; González, I.; González, F. J. *J. Phys. Chem. A* **2003**, *107*, 11161. (b) Gómez, M.; González, I.; González, F. J.; Vargas, R.; Garza, J. *Electrochem. Commun.* **2003**, *5*, 12.

(49) Matus, M. H.; Garza, J.; Galván, M. *J. Chem. Phys.* **2004**, *120*, 10359.

(50) Salvador, P.; Fradera, X.; Duran, M. *J. Chem. Phys.* **2000**, *112*, 10106.

(51) Hupp, T.; Engels, B.; Görling, A. *J. Chem. Phys.* **2003**, *119*, 11591.